On the Mechanism of the Single-Nucleon Knock-Out Reaction Induced by Pions at Medium Energies

by **L. C. Liu** and **P. Huguenin**

Institut de Physique, Université de Neuchâtel, Suisse

(15. XI. 72)

Abstract. A model for the knock-out reaction induced by pions at medium energies is proposed. In this model, the pion is treated as a strongly absorbed particle and the effect of nuclear binding is included in a simple way. Good agreement with experiment is obtained.

1. Introduction

The single-nucleon knock-out reaction can be used to investigate the single-nucleon momentum distribution inside the target nucleus and the off-shell properties of the pion-nucleon scattering amplitude, provided that the reaction proceeds via a 'quasi-free' process. A process is called quasi-free when the nuclear binding plays only a secondary role; such a process can also be termed quasi-elastic to emphasize the fact that no elementary particle has been created in the reaction.

The purpose of this paper is to examine the reaction mechanism of the single-nucleon knock-out reaction due to pions. Our aim is to investigate the possibility of using this reaction to study the off-shell properties of pion-nucleon scattering amplitude. The experimental data used in our analysis come from the reaction $^{12}C(\pi^+, \pi^+ p)^{11}B$ measured by Bellotti et al. [1–3] at about 130 MeV incident kinetic energy in laboratory.

In Section 2 the reaction model is elaborated while the explicit theoretical formulae used for numerical computation can be found in Section 3. Finally, the results are discussed in Section 4. We use the system of units with $\hbar = c = 1$.

2. Reaction Mechanism

2.1. *Survey of experiment and basic assumptions*

The pion beam energy in the above experiment ranged from 115 to 150 MeV in the laboratory system; and we assumed an average value of 132 MeV in our calculation. The two peaks shown by their 'missing energy' spectrum [1] are consistent with the separation energies of $1p$ and $1s$ protons of carbon obtained in $(p, 2p)$ and $(e, e'p)$ experiments [4, 5]. However, the final state of ^{11}B was not identified.

Nevertheless, the 'quasi-free' feature of the reaction is still visible. In Figures 1 and 2 we compare the knock-out reaction $^{12}C(\pi^+, \pi^+ p)\,^{11}B$ due to the $1p$ shell proton with the free pion–proton elastic scattering in the laboratory system. We see that:

1) The events of the reaction $^{12}C(\pi^+, \pi^+ p)\,^{11}B$ in the region corresponding to forward angles of the free pion–proton scattering are strongly suppressed.
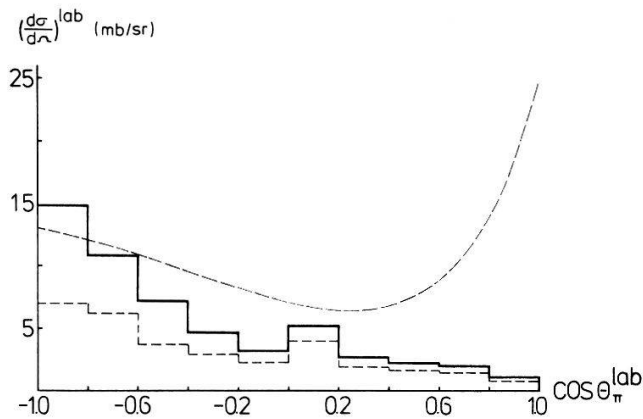
Figure 1

Angular distribution of final pions (lab. system). Incident $T_\pi^{lab} = 132$ MeV. Solid histogram: Untruncated experimental data of $^{12}C(\pi^+, \pi^+ p)\,^{11}B$ due to knocking out $1p$ shell protons [2]. Dashed histogram: Truncated experimental data, the events with a recoil ^{11}B momentum lower than 80 MeV/c are excluded [3]. Dashed curve: Free pion–proton elastic scattering with the target proton at rest.
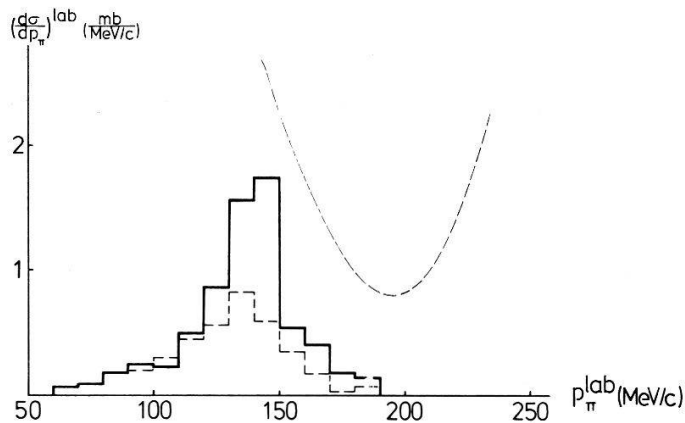
Figure 2

Cross-section as a function of final pion momentum (lab. system). Same caption as that in Figure 1.

2) Elsewhere, the events are in consistency with the picture in which the core nucleus ^{11}B behaves as if it were a mere spectator.

3) The peak of the final momentum distribution of pion is almost located in the same place as that of the backward peak of the free pion–proton elastic scattering.

We can therefore base our analysis on the following assumptions:

I) The knock-out reaction being studied can be regarded as a direct reaction whenever the energy transferred to the proton is sufficient.

II) The single scattering contribution is the dominant one for this channel.

2.2. Cross-section in distorted wave approximation

We are considering the transition amplitude from an incident pion and a target nucleus of A nucleons to an outgoing pion, an outgoing proton and a residual nucleus of $(A-1)$ nucleons. We use the subscripts 0 to denote the pion, 1 for the proton which interacts with the pion, A for target nucleus and c for the core nucleus.

Asymptotically, the final state wave function in the configuration space is, up to a numerical factor $\sqrt{A}$, due to antisymmetrization, given by

$$\Phi_f = \frac{1}{(2\pi)^{9/2}} e^{i(\vec{k}_0 \cdot \vec{r}_0 + \vec{k}_1 \cdot \vec{r}_1 + \vec{k}_c \cdot \vec{r}_c)} \varphi_c^{(\beta')}(\xi) \tag{2.1}$$

while that of the initial state can be expressed as

$$\Phi_i = \frac{1}{(2\pi)^3} e^{i(\vec{k}_0 \cdot \vec{r}_0 + \vec{k}_A \cdot \vec{r}_A)} \sum_{\alpha,\beta} \mathscr{A}(G_{\alpha\beta} \eta_1^{(\alpha)}(\vec{r}_{1c}) \varphi^{(\beta)}(\xi)). \tag{2.2}$$

The spin–isospin part of the wave functions is not explicitly written in order to simplify the notation. In the expressions (2.1) and (2.2), $\varphi_c^{(\beta)}$ is the antisymmetrized core wave function in a state β, $\eta_1^{(\alpha)}$ is the bound state proton wave function with the quantum number α. The product wave function in Φ_i is further properly antisymmetrized with the aid of the operator $\mathscr{A}$ with respect to space, spin and isospin variables.

We use the single-particle shell model description for carbon in our calculation, in this case

$$\mathscr{A}(G_{\alpha\beta} \eta_1^{(\alpha)}(\vec{r}_{1c}) \varphi_c^{(\beta)}(\xi)) \cong F_{\alpha\beta} \cdot C_{(1c)A} \eta_1^{(\alpha)}(\vec{r}_{1c}) \varphi_c^{(\beta)}(\xi)$$

where $C_{(1c)A}$ represents the Clebsch–Gordan coefficient performing the coupling of angular momenta, spins and isospins; and $F_{\alpha\beta}$ is the so-called generalized coefficient of fractional parentage [6].

The differential cross-sections that we are going to calculate can be obtained from the following formula:

$$\frac{d^9\sigma}{d^3\vec{k}_0' \, d^3\vec{k}_1' \, d^3\vec{k}_c'} = \sum_{\substack{\text{spin}\\\text{isospin}}} \frac{(2\pi)^4}{v_{in}} \delta^{(3)}(\sum_j \vec{k}_j' - \sum_j \vec{k}_j) \delta(E_f - E_i) |T_{fi}^{dir} + T_{fi}^{n.dir}|^2. \tag{2.3}$$

In relativistic kinematics

$$\frac{1}{v_{in}} = \frac{E_0 E_A}{\sqrt{(E_0 E_A - \vec{k}_0 \cdot \vec{k}_A)^2 - m_0^2 m_A^2}}.$$

As the non-direct part of the amplitude (2.3), which is related to the motion of residual nucleus, turns out to be very small at medium energies, we neglect it. In distorted wave approach the direct part is given by [6]

$$T_{fi}^{dir} = \langle \chi_f^{(-)} | t_{01} | \chi_i^{(+)} \rangle, \tag{2.4}$$

where $\chi_i^{(+)}$ and $\chi_f^{(-)}$ represents respectively the distorted waves in incoming and outgoing channel; and

$$t_{01}(E) = V_{01} + V_{01} \frac{1}{E + i\epsilon - K_0 - K_1 - K_c - V_{0c} - V_{1c} - h_c} V_{01} \tag{2.5}$$

The K_i stands for the kinetic energy operator of the ith 'particle' and the V_{jk} represents the two-body interaction between the jth and the kth 'particle'. The internal Hamiltonians are defined by

$$h_c \varphi_c^{(n)} = E_c^{(n)} \varphi_c^{(n)}, \quad h_A \varphi_A^{(m)} = E_A^{(m)} \varphi_A^{(m)}. \tag{2.6}$$

The operator t_{01} describes actually the scattering of the pion by the struck proton via interaction V_{01} in the presence of the core potentials V_{0c} and V_{1c}. For the purpose of the present paper, we simply use the impulse approximation which consists in replacing t_{01} by

$$\check{t}_{01}(E) = V_{01} + V_{01} \frac{1}{E + i\epsilon - K_0 - K_1 - K_c - h_c} V_{01}. \tag{2.7}$$

When this operator acts on the free wave (2.1), a simple energy shift takes place in the denominator and (2.7) becomes the free pion–proton operator with the corresponding free-particle state energy which we shall denote by w.

2.3. Surface reaction model

We know from pion–carbon elastic scattering that ^{12}C behaves almost as a 'black' target with respect to pions having a kinetic energy around 150 MeV in the laboratory [7]. Consequently, the pion can be regarded as a strongly absorbed particle in the sense that the inelasticity is large for all the low partial waves in the pion–carbon relative motion.

In view of the experimental evidence indicating that a dominant role may be played by single scattering process (Section 2.1), we divide the target nucleus into two regions. In the inner region where multiple collisions dominate we set the distorted pion waves to zero while in the outer region we use a plane wave. The cut-off radius is evaluated by using the following relation which connects the number N' of collisions with the elastic scattering phase shifts δ_l in the eikonal approximation:

$$N' = \sigma_{\pi N} \int_{-\infty}^{+\infty} \rho(\vec{b}, s) \, ds = \frac{4\pi}{k} \mathrm{Im}(f_{\pi N}(0)) \int_{-\infty}^{+\infty} \rho(\vec{b}, s) \, ds = \int_{-\infty}^{+\infty} \frac{-\mathrm{Im}\, U(\vec{b}, s)}{k} \, ds = 4\,\mathrm{Im}\,\delta_l$$

hence

$$|S_l| = |e^{2i\delta_l}| = e^{-2\mathrm{Im}\delta_l} = e^{-N'/2}. \tag{2.8}$$

In Figure 3 the $|S_l|$ obtained in a phase shift analysis for pion-carbon elastic scattering [7] are plotted against the impact parameter b $(l = kb - \frac{1}{2})$. The cut-off parameter R_c is taken as 2.75 fm. This large value of R_c means that the direct reaction takes place mainly in the peripheral region where the nuclear density is low. It has been noted that at medium energies the pion-nucleus interaction can be represented by a local one [8]. Consequently the pion-nucleon interaction inside the nucleus can be described by a contact one. This locality, together with our surface reaction model, enables us to use a plane wave for the final proton.

We have in the simple surface reaction model the following expression:

$$\frac{d^9 \sigma}{d^3 \vec{k}_0' \, d^3 \vec{k}_1' \, d^3 \vec{k}_c'} = \frac{(2\pi)^4}{v_{\mathrm{in}}} \delta^{(3)}(\sum_i \vec{k}_i' - \sum_i \vec{k}_i) \, \delta(E_f - E_i) \sum_{s'} |\sum_{s,j} \langle \vec{k}_0', \vec{k}_1', s' | \check{t}_{01}(w) | \vec{k}_0, \vec{k}_1, s \rangle$$

$$\times \sqrt{A} \, F_{(nlj,\beta')} \, C_{(1c)A} \, \tilde{\eta}_{ljm}^{\mathrm{cut}}(\vec{p}, s)|^2 \tag{2.9}$$

where the cut-off Fourier transform is defined by

$$\tilde{\eta}_{ljm}^{cut}(\vec{p}, s) = \frac{1}{(2\pi)^{3/2}} \int\limits_{R_c}^{\infty} e^{-i\vec{p}\cdot\vec{r}} \, \eta_{ljm}(\vec{r}, s) \, d^3\vec{r}. \tag{2.10}$$

In expression (2.9) s and s' stand for the spin-isospin variables. The subscript β' specifies the final state of core nucleus, moreover, the subscript of η_1 in (2.2) is now replaced by (ljm).
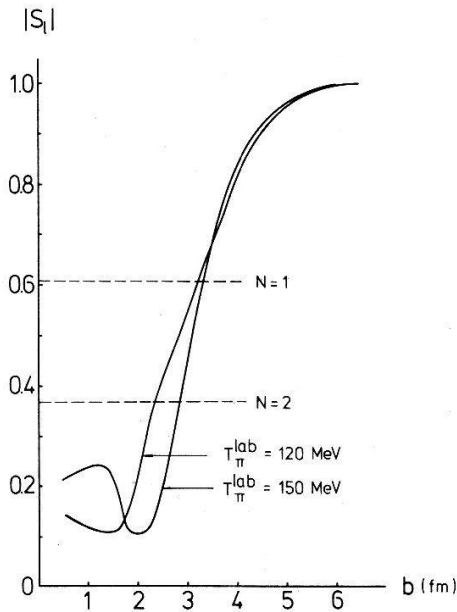

Figure 3

$|S_l|$ of $\pi^- - {}^{12}C$ elastic scattering as a function of impact parameter b.

The surface reaction model was proposed initially by Butler [9] for deuteron stripping reaction. Owing to the presence of three bodies in the final state of the knock-out reaction, some further thought must be given in treating the emission of the struck proton.

2.4. Binding effect consideration

The expression (2.9) is not satisfactory. The most serious shortcoming is that it does not contain any criterion indicating the effect of the binding on the struck proton. The physical picture is schematically represented by Figure 4.
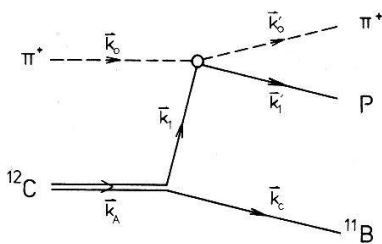

Figure 4

Schematic representation of impulse approximation.

The incoming pion encounters at the nuclear surface region a target proton having the momentum distribution of an actual bound state. After the direct interaction both pion and proton leave the residual nucleus to become free particles whatever the circumstance may be.

Actually, before and during the direct interaction the core potential V_{1c} is still strong enough to bind the proton. Owing to this nuclear binding, the struck proton cannot be ejected in a simple way unless its energy variation during the direct impulsive collision is larger than a threshold; for instance, the corresponding separation energy. We impose therefore the following condition:

$$\tilde{Q} < \left| \frac{p'^2}{2m_1^*} + V_{1c}(r) - \left(\frac{p^2}{2m_1^*} + V_{1c}(r) \right) \right| = \left| \frac{p'^2 - p^2}{2m_1^*} \right| \equiv \Delta T_p. \tag{2.11}$$

The p and p' are respectively the magnitudes of the proton momentum before and after the direct interaction, calculated in the c.m. system of proton-residual nucleus. The m_1^* is the reduced mass of the proton.

Consequently, we multiply the formula (2.9) by a step function defined by

$$\theta(\Delta T_p - \tilde{Q}) = 1 \quad \text{if } \Delta T_p > \tilde{Q}$$
$$= 0 \quad \text{otherwise} \tag{2.12}$$

The quantity $\tilde{Q}$ can be regarded as a free parameter, though in the present calculation it was chosen as equal with the separation energy (see appendix).

In summary, we are using a surface reaction model with an *ad hoc* binding correction

3. Calculation of the Differential Cross-Sections

For the sake of simple parametrization, we chose to compute in the over-all centre-of-mass system. The starting formula according to our model is then

$$\frac{d^9\sigma}{d^3\vec{k}'_0\, d^3\vec{k}'_1\, d^3\vec{k}'_c} = (2\pi)^4 \frac{E_0 E_A}{\sqrt{(E_0 E_A + k_0^2)^2 - m_0^2 m_A^2}} \delta^{(3)}(\vec{k}'_0 + \vec{k}'_1 + \vec{k}'_c)$$

$$\times \delta(E'_0 + E'_1 + E'_c - E_0 - E_A) \sum_{m'_s, M'} | \sum_{lmm_s} F_{(j)} \sqrt{A}$$

$$\times \langle \vec{k}'_0, \vec{k}'_1, m'_s | \check{t}_{01}(w) | \vec{k}_0, \vec{k}_1, m_s \rangle \frac{1}{\sqrt{2}} C^{j\,j\,0}_{-M'\,M'\,0} C^{l\,\frac{1}{2}\,j}_{m\,m_s\,-M'}$$

$$\times \tilde{\eta}^{\text{cut}}_{lm}(\vec{p}) \, \theta(\Delta T_p - \tilde{Q})|^2, \tag{3.1}$$

where

$$\vec{k}'_c = \vec{k}_c \quad \text{(Assumption I)}$$

$$\vec{k}_c + \vec{k}_1 = \vec{k}_A = -\vec{k}_0$$

and in the non-relativistic limit for proton-core nucleus system

$$\vec{p} = -\left(\frac{A-1}{A} \vec{k}_0 + \vec{k}_c \right)$$

The j is the spin of core nucleus and M' its z-component. The m'_s and m_s are z-components of the spin of the struck proton. The factor $1/\sqrt{2}$ is due to isospin coupling. The quantities $\eta^{cut}_{lm}(\vec{p})$ and ΔT_p are respectively defined by (2.10) and (2.11).

The harmonic oscillator wave function is used for the bound proton, its spatial part is given by

$$\eta_{lm}(\vec{r}) = \frac{1}{\pi^{1/4} R^{3/2}} \left(\frac{2^{l+2}}{(2l+1)!!} \right)^{1/2} \left(\frac{r}{R} \right)^l e^{-r^2/2R^2} Y^l_m(\Omega_r)$$ (3.2)

such that

$$\int d^3\vec{r}\, \eta^*_{l'm'}(\vec{r})\, \eta_{lm}(\vec{r}) = \delta_{ll'}\, \delta_{mm'}.$$

Among the nine variables at the left-hand side of the formula (3.1) only five of them are independent. By integrating over the 'unmeasured' variables, we obtain the various distributions in the pion-carbon centre-of-mass system, which can be easily transformed into the laboratory system with the aid of appropriate transformation jacobians. In our computation the limits of each integration are taken to be that given by kinematics.

To take the applied experimental condition [1] into account, we have excluded the part having a final proton kinetic energy lower than 10 MeV in the laboratory.

Since the main purpose of this paper is the investigation of the reaction mechanism, we did not make a fit. The values of the parameters used for computation are directly taken from the relevant experiments in literature (Table 1).

Table 1
Parameters used for computation

Parameters	Values	Remarks	Ref.
R_c	2.75 fm		Fig 3
$\tilde{Q}$	16 MeV	Separation energy for $1p$-proton in ^{12}C	[1], [4], [5]
R	1.678 fm	$\langle r^2 \rangle_{12C} = 2.47$ fm	[10]
$\sqrt{A}\, F_{(J)}$	$\sqrt{2(2j+1)}$	Closed sub-shell	

The off-shell free π^+-proton scattering amplitude in the formula (3.1) can be expressed in terms of the quantities defined in the c.m. system of π^+-proton:

$$\langle \vec{k}'_0, \vec{k}'_1, m'_s | \check{t}_{01}(w) | \vec{k}_0, \vec{k}_1, m_s \rangle = \left(\frac{E^{*'}_0 E^{*'}_1 E^*_0 E^*_1}{E'_0 E'_1 E_0 E_1} \right)^{1/2} \langle \vec{k}^{*'}, m'_s | \check{t}_{01}(w) | \vec{k}^*, m_s \rangle$$

with $E^{*2}_i = k^{*2} + m^2_i, \quad E^2_i = k^2_i + m^2_i, \quad i = 0, 1.$ (3.3)

We choose the energy parameter in $\check{t}_{01}(w)$ to be

$$w = \sqrt{s} = E^*_0 + E^*_1$$

and make the following parametrization:

$$\langle \vec{k}^{*'}, m'_s | \check{t}_{01}(w) | \vec{k}^*, m_s \rangle \propto \frac{1}{k^*} [(B_0 + B_1 \cos\theta^*)\, \delta_{m'_s, m_s}$$

$$- B_2 \sin\theta^* (\sqrt{\tfrac{3}{4} - m_s(m_s+1)}\, e^{-i\phi^*} \delta_{m'_s, m_s+1} \sqrt{\tfrac{3}{4} - m_s(m_s-1)}\, e^{i\phi^*} \delta_{m'_s, m_s-1})]$$ (3.4)

where the energy-dependent coefficients B_0, B_1 and B_2 are related to pion-nucleon phase shifts by

$$B_0 = a_{31}^0(\sqrt{s}) \tag{3.5a}$$

$$B_1 = a_{31}^1(\sqrt{s}) + 2a_{33}^1(\sqrt{s}) \tag{3.5b}$$

$$B_2 = a_{31}^1(\sqrt{s}) - a_{33}^1(\sqrt{s}) \tag{3.5c}$$

and

$$a_{2T,2j}^l(\sqrt{s}) = [\eta_{2T,2j}^l(\sqrt{s}) \exp(2i\delta_{2T,2j}^l(\sqrt{s})) - 1]/2i. \tag{3.5d}$$

The values of $\eta_{2T,2j}^l$ and $\delta_{2T,2j}^l$ as a function of $\sqrt{s}$ are obtained by interpolating the set of CERN fit [11].

In the right-hand side of the amplitude (3.4), the first term is the spin-nonflip contribution and the second term is the spin-flip contribution. The spin-flip amplitude is neither zero nor negligible. The interference terms disappear, however, after the azimuthal integration. We define the scattering angle θ^* to be the angle between the initial pion momentum $\vec{k}^*$ and final pion momentum $\vec{k}^{*\prime}$ in the centre-of-mass system of the π^+-proton.

4. Results and Discussions

The distributions given by our model are compared with the corresponding experimental data [2, 3] in Figure 5 through Figure 9. The agreement is good; especially as no free parameters were used in the calculations. In Figures 5 and 6 the PWIA results are also plotted for reference. It is worth mentioning that with respect to the PWIA results the surface reaction assumption alone caused a decrease in magnitude without appreciably changing the form of those curves. Our binding correction is therefore a vital ingredient.

The lower the incident energy of projectile the narrower is that part of the phase space region where the inequality (2.11) is fulfilled, and the more important becomes this binding correction. In order to test the importance of our binding correction at higher energies, we compared our theoretical results in Figure 8 with the measurement, due to Agan'yants et al. [12]. We see that even at a pion incident energy of 1 GeV this correction still changes appreciably the final pion momentum distribution and causes a significant shift of peak. Since in their counter experiment the high momentum tail of the final pion spectrum is free from experimental bias, we consider the improvement shown in Figure 8 as an indication that our binding correction represents a real simulation of the complicated reaction mechanism.

The unusual experimental backward peak in Figure 7 might come from the uncertainty in the separation of the pion-hydrogen events in the bubble chamber. This viewpoint is supported by the histogram excluding the events having a recoil ^{11}B momentum lower than 80 MeV/c in the laboratory, in which the backward peak is compatible with the theoretical result. Unfortunately, this truncation produces for each distribution an underestimated experimental value resulting from the simultaneous elimination of the real knock-out events having a low recoil ^{11}B momentum.

As to the treatment of pion distortion we note that a refinement can be achieved by using a smooth cut-off function in r-space. This function may be deduced from the
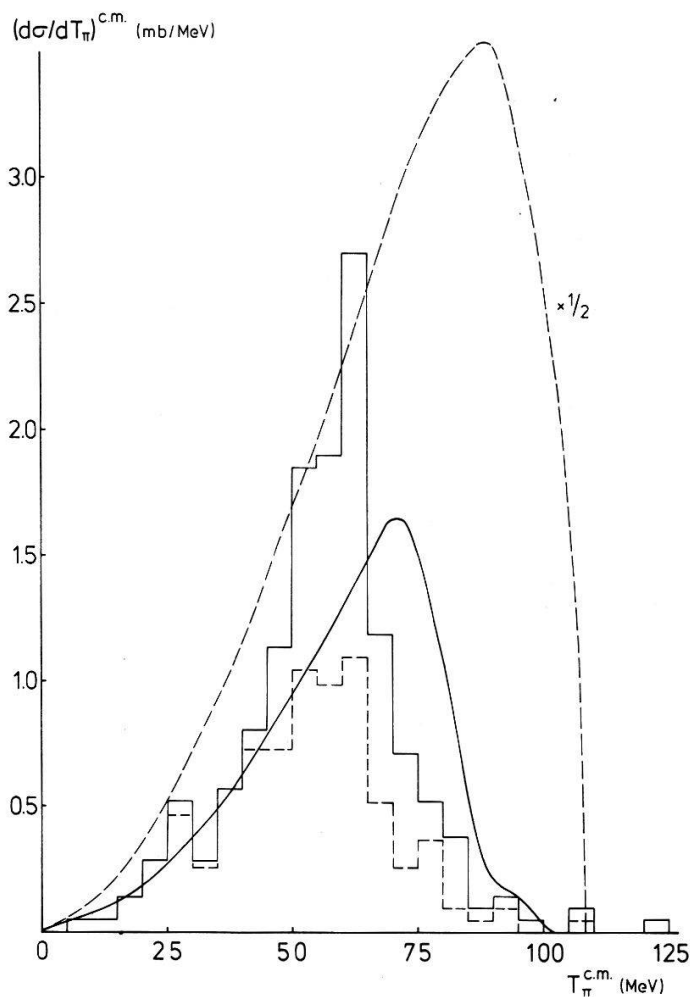
Figure 5

Cross-section as a function of final pion kinetic energy.

$(\pi^+ - {}^{12}\text{C}$ c.m. system; incident $T_\pi^{\text{lab}} = 132$ MeV.)

Solid histogram: Untruncated experimental data of ${}^{12}\text{C}(\pi^+, \pi^+ p)\,{}^{11}\text{B}$ due to knocking out $1p$ shell protons [2]. Dashed histogram: Truncated experimental data, the events with a recoil ${}^{11}\text{B}$ momentum lower than 80 MeV/c are excluded [3]. Solid curve: Result of this model. Dashed curve: PWIA multiplied by the indicated factor.
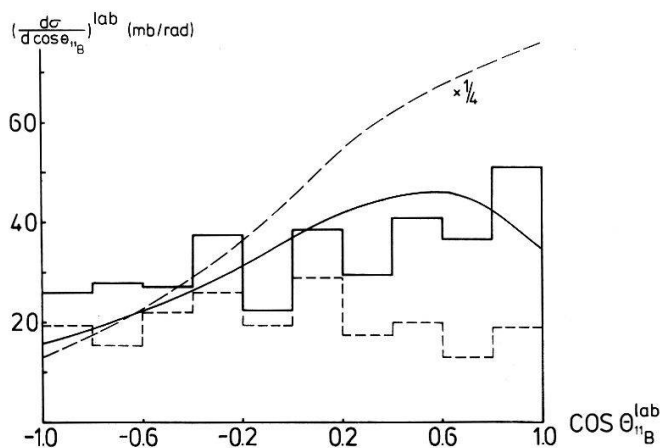

Figure 6

Angular distribution of ${}^{11}\text{B}$ (lab. system). Same caption as that in Figure 5.

shape of $|S_l|$ of the pion-carbon elastic scattering (Fig. 3). Although this will modify the theoretical curves, in particular the diffractive pattern in the momentum distribution of the residual nucleus, the essential of the reaction mechanism remains unchanged.

Another remark concerns the non-direct part of T_{fi} that we disregarded in Section 2.2. For a same final geometry the ejected proton has undergone an energy variation
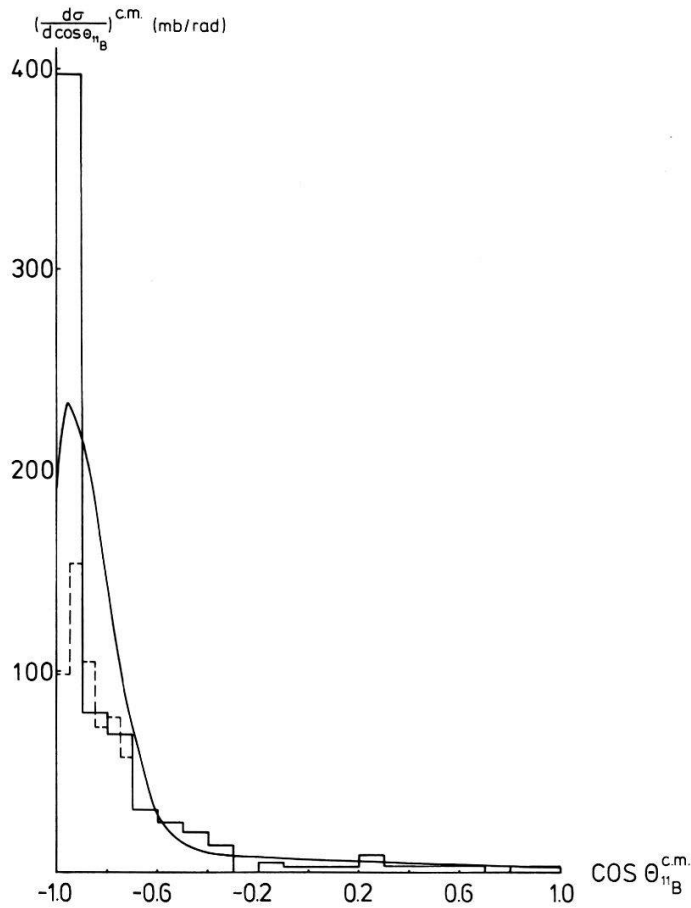

Figure 7

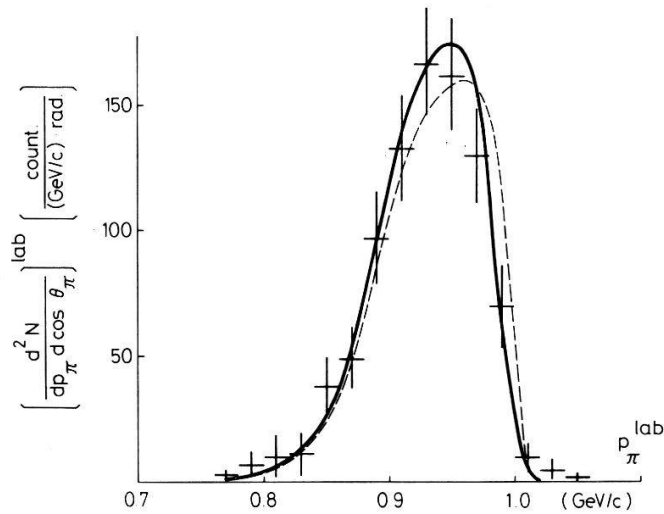Angular distribution of ^{11}B ($\pi^+ - {}^{12}$C c.m. system). Same caption as that in Figure 5.

Figure 8

Cross-section of ^{12}C$(\pi^-, \pi^- p)$ ^{11}B as a function of final pion momentum in lab.-system. $p_{\pi, \text{in}}^{\text{lab}} = 1.04$ GeV/c, $\theta_{\pi, \text{out}}^{\text{lab}} = 20.5°$ [12]. Curves are normalized to experimental data. Dashed curve: PWIA result. Solid curve: PWIA + binding correction.

only equal to $1/(A-1)$ of that involved in T_{fi}^{dir}. Consequently, a binding correction like (2.11) makes the contribution due to $T_{fi}^{n\cdot dir}$ negligibly small.

In view of the success of our model we may conclude that the knock-out reaction induced by pions at these incident energies proceeds mostly via a quasi-free process.
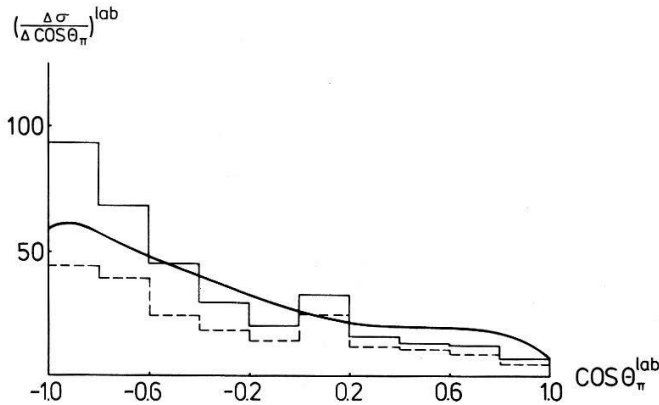

Figure 9
Angular distribution of the final pions (lab. system). Same caption as that in Figure 5.

Therefore, it is hopeful that some information about off-shell pion-nucleon scattering amplitude could be obtained by measuring a single nucleon knock-out reaction in a kinematical domain in favour of 'quasi-free' process.

5. Acknowledgment

APPENDIX

Nuclear Break-up Condition in the Framework of Impulse Approximation

In our model a binding correction has been introduced to simulate the complicated reaction mechanism in connection with the emission of the struck proton by the target nucleus.

According to Figure 4 the energy variation of the system struck proton–core nucleus during the impulsive collision between the projectile and the struck proton is

$$D = (T_{1c}' - T_{1c}) + (T_A' - T_A) = D^{rel} + D^{c.m.},$$

where T_{1c} is the relative kinetic energy of proton to core nucleus and T_A is the kinetic energy associated to the motion of centre-of-mass of proton and core nucleus. Our conjecture is that the struck proton will not be emitted in a simple way unless the energy variation related to this emission is larger than the characteristic energy binding the proton in the core nucleus, i.e.

$$\Delta T_p \equiv |D^{rel}| > | <h_{1c}> | \equiv \tilde{Q}$$

with the Hamiltonian defined by

$$h_{1c} = h_A - h_c.$$

The quantity $\tilde{Q}$ is therefore related to the wave function of the target nucleus. In the single-particle shell model description we obtain for $\tilde{Q}$ the following value:

$$\tilde{Q} = |<h_{1c}>| = |<\phi_A^{(0)}|h_{1c}|\phi_A^{(0)}>| = E_{\text{separation}},$$

where $\phi_A^{(0)}$ is the ground state wave function of the target nucleus.

REFERENCES

[1] E. BELLOTTI and S. BONETTI, *Proceedings of the Topical Seminar on: "Interaction of Elementary Particles with Nuclei", Trieste 1970*, edited by G. BELLINI, L. BERTOCCHI and S. BONETTI (I.N.F.N., 1970), p. 369.

[2] E. BELLOTTI, D. CAVALLI and C. MATTEUZZI, private communications.

[3] E. BELLOTTI, S. BONETTI, D. CAVALLI and C. MATTEUZZI, Preprint (I.N.F.N.) (to be published in Nuovo Cimento).

[4] H. TYREN, S. KULLANDER, O. SUNDBERG, R. RAMACHANDRAN, I. ISACSSON and T. BERGGREN, Nucl. Phys. *79*, 321 (1966).

[5] U. AMALDI, JR., G. CAMPOS VENUTI, G. CORTELLESSA, C. FRONTEROTTA, A. REALE, P. SALVADORI and P. HILLMAN, Phys. Rev. Letters *13*, 341 (1964).

[6] T. BERGGREN, Ann. Rev. Nucl. Sci. *16*, 153 (1966).

[7] J. BEINER, University of Neuchatel, Switzerland (preprint to be submitted to Nuclear Physics).

[8] C. WILKIN, *SIN-CERN Spring School on Pion Interactions at Low and Medium Energies*, CERN Report, 71–14, p. 315.

[9] S. T. BUTLER, in *Nuclear Stripping Reactions* (John Wiley & Sons, Inc., New York 1957).

[10] H. R. COLLARD, L. R. B. ELTON AND R. HOFSTADTER, in *Nuclear Radii*, Landolt-Börnstein New Series, Vol. I/2, edited by H. SCHOPPER (Springer Verlag, Berlin-Heidelberg-New York 1968), p. 32.

[11] D. J. HERNDORN et al., *π-N Partial-Wave Amplitudes*, Lawrence Radiation Laboratory Report, UCRL-20030 (1970), p. 79.

[12] A. O. AGAN'YANTS, YU. D. BAYUKOV, V. N. DEZA, S. V. DONSKOV, V. B. FEDOROV, N. A. IVANOVA, V. D. KHOVANSKY, V. M. KOLYBASOV, G. A. LEKSIN, V. L. STOLIN and L. S. VOROBYEV, Nucl. Phys. *B11*, 79, Fig. 12(a) + 12(b) (1969).